Catalysis Today 148 (2009) 341–349

Contents lists available at ScienceDirect

Catalysis Today

journal homepage: www.elsevier.com/locate/cattod

CO_2 reforming into fuel using TiO_2 photocatalyst and gas separation membrane

Akira Nishimura [a,*], Nobuyuki Komatsu [a], Go Mitsui [a], Masafumi Hirota [a], Eric Hu [b]

[a] Division of Mechanical Engineering, Graduate School of Engineering, Mie University, 1577 Kurimamachiya-cho, Tsu, Mie 514-8507, Japan
[b] School of Mechanical Engineering, The University of Adelaide, SA 5005, Australia

ARTICLE INFO

Article history:
Available online 3 August 2009

Keywords:
TiO_2 photocatalyst
CO_2 reforming
Membrane reactor
Gas separation membrane
Sol–gel and dip-coating method

ABSTRACT

It was previously reported that CO_2 could be reformed into CO, CH_4, etc., which can be used as fuels, by TiO_2 as the photocatalyst and under UV radiation. If this technique could be applied practically, a carbon circulation system would then be able to be constructed by reforming CO_2 from combustion, using solar energy, to fuel, which would solve the problem of global warming and fossil fuels depletion all together. However, the technology is not yet practicable as the fuel concentration of products is too low. To increase the concentration and improve CO_2 reforming performance on TiO_2, a membrane reactor composed of TiO_2 and gas separation membrane prepared by sol–gel and dip-coating method has been built. Study on the factors influencing membrane performance, e.g. rising speed in the dip-coating process, has been carried out with the reactor. The results of the study are reported in this paper.

1. Introduction

Due to mass consumption of fossil fuels, global warming and fossil fuels depletion have become the serious global environmental problems in the world. After the industrial revolution, the averaged concentration of CO_2 in the world has been increased from 280 ppmV to 383 ppmV. Therefore, it is necessary to develop new energy production technologies with less or no CO_2 emission.

It is reported that CO_2 can be reformed into fuel of CO, CH_4, CH_3OH, H_2, etc., by TiO_2 photocatalyst under UV illumination [1–11]. If this technique could be applied practically, a carbon circulation system would then be able to be constructed by reforming CO_2 from combustion, using solar energy, to fuel, which would solve the problem of the global warming and fossil fuels depletion all together. Many works on this technology have been carried out, but mainly for the experimental systems that TiO_2 particle loaded with Cu, Pd, Pt reacts with CO_2 dissolved in solution [5,7,8,12–18]. Recently, nano-scale TiO_2 [19–21], porous shape TiO_2 [22], TiO_2 film combined with metal [23,24], and dye sensitized TiO_2 [25,26], are developed for this process. However, the fuel concentration in the products is still low ranging from 10 ppmV to 1000 ppmV [5,7,8,10–14,18,19,21]. For the fuel is able to be used practically, the lowest combustible concentration, for example, for CH_4 and CO is 5.3 vol.% and 12.5 vol.%, respectively. Therefore, the big breakthrough is necessary to improve the CO_2 reforming performance.

To improve CO_2 reforming performance, our previous works were concentrated on the preparation of the TiO_2. We have adopted the sol–gel and dip-coating method for the preparation of TiO_2 film. In our former papers [27–31], we reported the investigation of the effect of TiO_2 film preparation conditions such as coating number of film (*N*), firing duration time (*FD*) and firing temperature (*FT*) in the drying process of dip-coating method, and ratio of added TiO_2 powder to the amount of TiO_2 in sol solution on CO_2 reforming performance. In addition, we also studied the effect of metal deposition on TiO_2 film because it was thought that the metal deposition on TiO_2 film would prevent the recombination of hole and electron produced in reaction from the other report on TiO_2 photocatalyst study [7]. Cu, Pd and Pt were selected for the metal deposition. With investigating the performances of these TiO_2 film in the batch reactor which was filled with CO_2 gas and water vapor, the concentration of reforming product was increased up to 3 vol.% as the maximum [27–31]. This increase is due to the increase in the reaction surface area of TiO_2, good arrangement of thickness of TiO_2 film, upgrading TiO_2 crystallization, and preventing recombination of electron and hole by loaded metal. However, it is necessary to further improve if the products are to be used as fuel. In this study, the new approach, which is different from the previous approaches focusing on the preparation method of TiO_2 film, has been undertaken.

According to the calculation by the author, the mass transfer time of 10^5 s to 10^{-1} s is slower than the photo reaction time of 10^{-9} s to 10^{-15} s. Therefore, it is thought that the mass transfer is the inhibition factor to speed up photocatalyst reaction. Another reason courses the low reforming rate is the re-oxidization of the products. Namely, due to the reaction surface covered by products,

* Corresponding author. Tel.: +81 59 231 9747; fax: +81 59 231 9747.
E-mail address: nisimura@mach.mie-u.ac.jp (A. Nishimura).

0920-5861/$ – see front matter © 2009 Elsevier B.V. All rights reserved.
doi:10.1016/j.cattod.2009.07.067

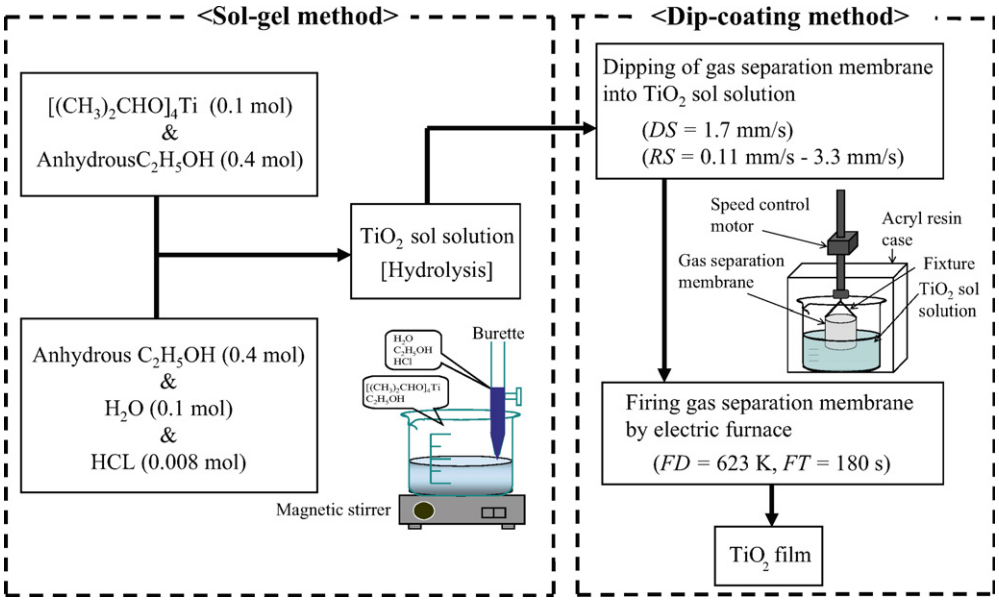

Fig. 1. Sol–gel and dip-coating method to prepare TiO_2 film in this study.

the movement of the reactants to the reaction surface is prevented and the reverse reaction, i.e. re-oxidization, which reproduces CO_2 from CO and CH_4 is occurred. Therefore, it is desirable that the products, i.e. CO and CH_4 are removed from the reaction surface as soon as they are produced, so that the reactants, i.e. CO_2 and water vapor can continue to react on the reaction surface. Fuel production can be sustained by maintaining the non-equilibrium reaction state.

The gas separation membrane is usually used for the gas separation process like H_2 production from hydrocarbon, O_2 enrichment from the air, and CO_2 capture of the industrial power plants. Since the molecular diameters of reactant of CO_2 and water vapor are smaller than that of CO and CH_4 (CO_2: 0.33 nm, water vapor: 0.28 nm, CH_4: 0.38 nm, CO: 0.38 nm) [32–34], the promotion of mass transfer by gas separation is thought to be possible and was attempted in this study. This is a novel approach to improve CO_2 reforming performance over the TiO_2. No similar attempts have been reported yet.

The aim of this study is to investigate the effect of mass transfer promotion and maintaining non-equilibrium reaction state by separating product from reactant on CO_2 reforming performance of TiO_2.

The rising speed (*RS*) of gas separation membrane from the TiO_2 sol solution in dip-coating process, which influences the thickness and physical and chemical structure of TiO_2 film prepared on the gas separation membrane, is in the range of 0.11–3.3 mm/s, in this study. The surface structure and crystallization characteristics of TiO_2 film on gas separation membrane, prepared by different *RS* are analyzed by SEM (Scanning Electron Microscope, JXA8900R, JEOL Ltd.) and EPMA (Electron Probe Micro Analyzer, JXA8900R, JEOL Ltd.) in order to understand the relationship between *RS* and the surface structure and crystallization characteristics of TiO_2 film, as the first step in this study. CO_2 reforming and permeation performance of TiO_2 film coated on gas separation membrane is evaluated firstly in the batch type reactor to select the TiO_2 film coating condition which is thought to be suitable for the membrane reactor of gas circulation type. In other words, the ideal TiO_2 film for this application should have large reaction surface areas and high crystallization characteristics but does not block the pores of gas separation membrane. After that, TiO_2 film on the gas separation membrane is investigated in a reactor of gas circulation type. The effect of gas separation and circulation on CO_2 reforming performance is verified by comparing it with the results obtained from the batch type reactor.

2. Experimental

2.1. Preparation method of TiO_2 film coated on gas separation membrane

Sol–gel and dip-coating method was used for preparing TiO_2 film in this study. Fig. 1 represents the flow chart of the sol–gel and dip-coating method. TiO_2 sol solution was made by mixing $[(CH_3)_2CHO]_4Ti$ (purity of 95 wt.%, Nacalai Tesque Co.), anhydrous C_2H_5OH (purity of 99.5 wt.%, Nacalai Tesque Co.), distilled water, and HCl (purity of 35 wt.%, Nacalai Tesque Co.). The gas separation membrane (silica–alumina gas separation membrane, Noritake Co., Ltd.), which was the porous multilayer ceramic tube shown in Fig. 2, was dipped into TiO_2 sol solution and pulled up at the fixed speed. Then, it was dried out and fired under the controlled *FT* and *FD*, resulting that TiO_2 film was fastened on the surface of gas separation membrane. *N* was fixed at 1. *FT* and *FD* was set 623 K and 180 s, respectively. *RS* varied from 0.11 mm/s to 3.3 mm/s.

Fig. 2. Gas separation membrane.

Table 1
Physical properties of gas separation membrane.

	Thickness [μm]	Mean pore size [nm]	Void ratio [−]	Permeability [m^2]
(1) Silica (SiO_2) layer	0.2	0.4	0.27	5.44×10^{-22}
(2) γ-Alumina (Al_2O_3) layer	2	4	0.44	8.88×10^{-20}
(3) α-Alumina (Al_2O_3) layer	100	60	0.39	1.76×10^{-17}
(4) α-Alumina (Al_2O_3) supporter	1000	700	0.40	2.45×10^{-15}

Silica layer is the top layer of this gas separation membrane. γ-Alumina layer is the second layer. α-Alumina layer is the third layer. α-Alumina supporter is the bottom layer of gas separation membrane.

Downing speed (*DS*) of gas separation membrane into TiO_2 sol solution in dip-coating process was kept at the constant speed of 1.7 mm/s. Table 1 lists the physical properties of the gas separation membrane. It can be seen, the mean pore size of silica layer is not between the molecular diameter of reactants and that of products, as required. It is difficult to find the gas separation membrane with the ideal pore size. However, the gas separation membrane selected is capable of separating gases through both molecular sieving diffusion and so called Knudsen diffusion mechanisms, therefore it can be used in this study. The Knudsen diffusion can separate the gases though the pore size of silica layer is larger than the molecular diameter of gas to be separated. Since the molecular diameter of reactant and that of product is actually different as described above, we have decided to adopt this gas separation membrane.

The TiO_2 films prepared were observed by SEM to evaluate the influence of *RS* on their surface structures. In addition, they were analyzed by EPMA to understand the influence of *RS* on crystallization characteristics of TiO_2 film coated on gas separation membrane.

2.2. Experimental apparatus and procedure

Fig. 3 illustrates the CO_2 reforming reactor that is termed as CO_2 reformer, with TiO_2 film coated on gas separation membrane. This reactor consists of one gas separation membrane with TiO_2 film (150 mm (*L*) × 6 mm (*O.D.*) × 1 mm (*t*), whose reaction surface area is equal to the outer surface area: 2.26×10^{-3} m^2 and gas

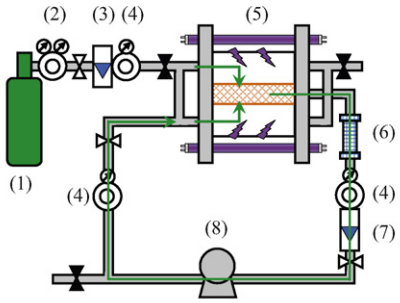

(1) CO_2 gas cylinder (99.995 vol%) (2) Regulator (3) Mass flow controller
(4) Pressure gauge (5) CO_2 reformer (6) Gas drier (Silica gel)
(7) Mass flow meter (8) Tube pump

Fig. 4. CO_2 reforming and permeation experiment system.

filling volume: 2.88×10^{-4} m^3), one quartz glass tube (266 mm (*L*) × 42 mm (*O.D.*) × 2 mm (*t*)), and four UV lamps (FL16BL/400T16, Raytronics Corp., 400 mm (*L.*) × 16 mm (*D.*)) located at 20 mm apart from the surface of gas separation membrane symmetrically. These parts are assembled with stainless plates by bolts and nuts. The center wave length and mean light intensity of UV light illuminated from every UV lamp is 365 nm and 2.4 mW/cm^2, respectively. This is similar to the average light intensity level of UV ray in solar radiation in the daytime through the year.

Fig. 4 illustrates the whole experimental system set-up, which is termed as membrane reactor. With this membrane reactor, not only batch type but also gas circulation type experiment can be conducted. When it is used for batch type experiment, the valves located at inlet and outlet of CO_2 reformer are closed. The membrane reactor is composed of CO_2 reformer, CO_2 gas cylinder, mass flow controller (MODEL3660, KOFLOC), mass flow meter (CK-1A, KOFLOC), pressure gauge, gas drier and tube pump (WM-520S/R2, Iwaki Pumps).

In the CO_2 reforming experiment by the batch type reactor, CO_2 gas whose purity was 99.995 vol.% was flowed through the CO_2 reformer as a purged gas for 15 min at first. After that, the valves located at inlet and outlet of CO_2 reformer were closed. After

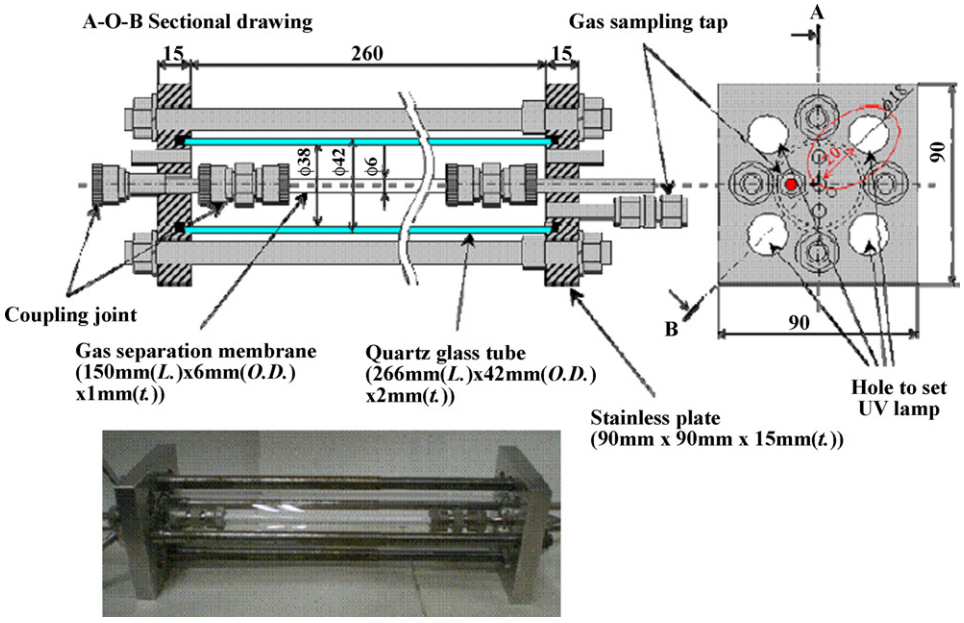

Fig. 3. CO_2 reformer composed of TiO_2 film coated on gas separation membrane. (UV lamp is removed from this figure for understanding the inside of CO_2 reformer.)

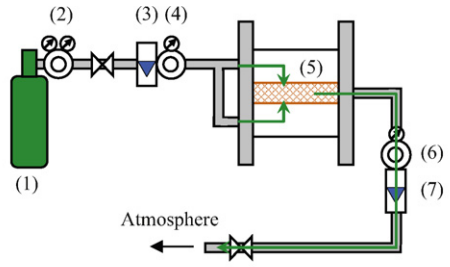

(1) CO_2 gas cylinder (2) Regulator (3) Mass flow controller

(4) Pressure gauge (5) Gas separation membrane (6) Pressure gauge

(7) Mass flow meter

Fig. 5. Arranged CO_2 reforming and permeation experimental system for CO_2 permeation experiment.

confirming the gas pressure and gas temperature in the reactor at 0.1 MPa and 298 K, respectively, the distilled water of 1.00 mL (55.6 mmol) was injected into the CO_2 reformer and UV light illumination was started at the same time. This water was vaporized after injected into the reformer. Despite the heat of UV lamp, the temperature in CO_2 reformer was kept about 353 K during the CO_2 reforming experiment. The amounts of the injected water and the CO_2 in the batch type reactor are 55.6 mmol and 13.0 mmol, respectively. The gas in CO_2 reformer was sampled every 24 h in CO_2 reforming experiment. The sampled gas was analyzed by FID gas chromatograph (GC353B, GL Science) and methanizer (MT221, GL Science). In this experiment, only CO was detected as the product.

In the CO_2 permeation experiment, the CO_2 reforming and permeation experimental system shown in Fig. 4 was arranged. Fig. 5 illustrates the arranged CO_2 reforming and permeation experimental system for CO_2 permeation experiment by batch type. In the CO_2 permeation experiment, the CO_2 permeation flux was measured under the condition that the absolute pressure and temperature of supply gas to the apparatus was 0.10–0.38 MPa and 298 K, respectively. The flow rate of supply gas was set 500 mL/min by mass flow controller. The flow rate of permeation gas was measured by mass flow meter.

In the CO_2 reforming experiment carried out by the membrane reactor of gas circulation type, UV light was being illuminated under the same condition of batch type reactor until the steady reaction state was confirmed. After that, the gas circulation by tube pump was started. The suction pressure and flow rate of permeation gas was controlled to evaluate the effect of gas separation and circulation on CO_2 reforming performance of this membrane reactor. The produced CO would be removed from the CO_2 reformer to outside of the system by switching the outlet valve of CO_2 reformer on and off when needed. The distilled water of 1.00 mL was injected into CO_2 reformer when the CO_2 reforming experiment under the condition of batch type reactor was established. The gas sampled every 24 h from CO_2 reformer was analyzed by FID gas chromatograph and methanizer.

3. Results and discussion

3.1. Analysis result of TiO_2 film coated on gas separation membrane by SEM and EPMA

Fig. 6 shows SEM images of TiO_2 film prepared under conditions of different several *RS*. These SEM images are taken by 200 times and 1500 times magnification under the condition of acceleration voltage of 15 kV and current of 3.0×10^{-8} A. There is no cluck for TiO_2 film prepared seen if *RS* is below 0.22 mm/s, indicating a successful uniform coating. There is cluck, which becomes larger with the increase of *RS* in the range from *RS* = 0.33 mm/s to *RS* = 1.1 mm/s. The gap, which contains part of large clucks and condensed TiO_2 film, is observed and becomes larger when the *RS* is over 1.1 mm/s. Although it is known that the formation of the suitable sized clucks has positive effect on CO_2 reforming promotion [28,31], the expansion of gaps area also causes the decrease in the reaction surface area of TiO_2 film and weakens the fastening force acted on gas separation membrane. Generally speaking, the thickness and roughness of TiO_2 film prepared by sol–gel and dip-coating method becomes larger with the increase of *RS*. Moreover, the thermal stress acted on the interface between

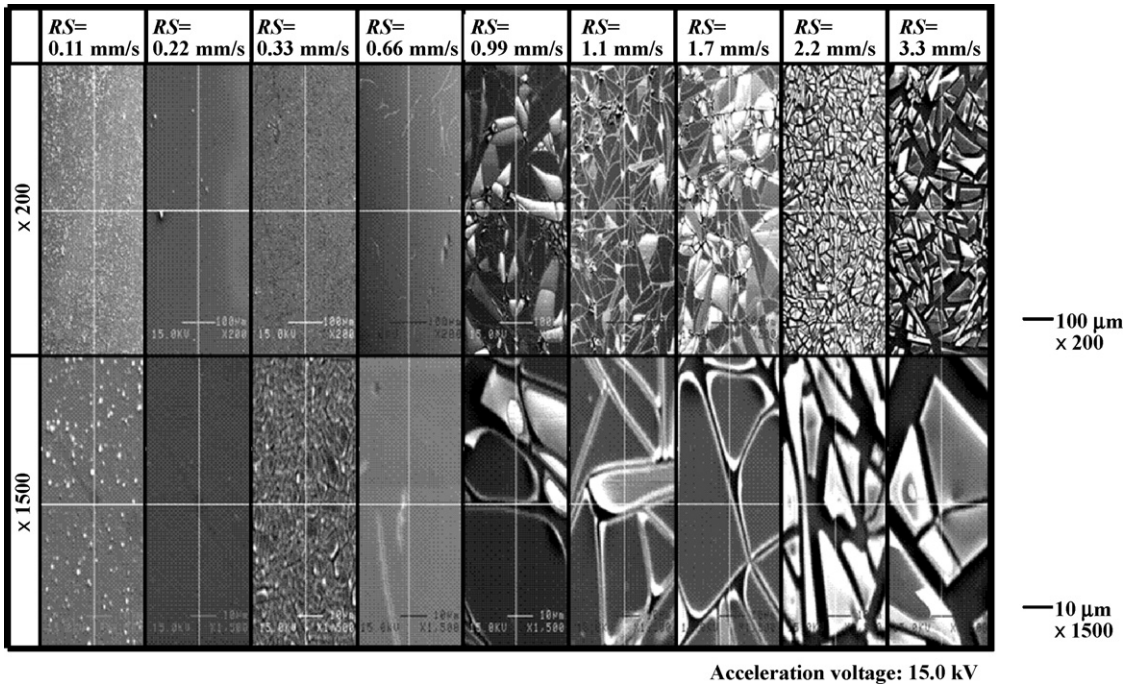

Fig. 6. SEM images of TiO_2 film prepared under conditions of different several *RS*.

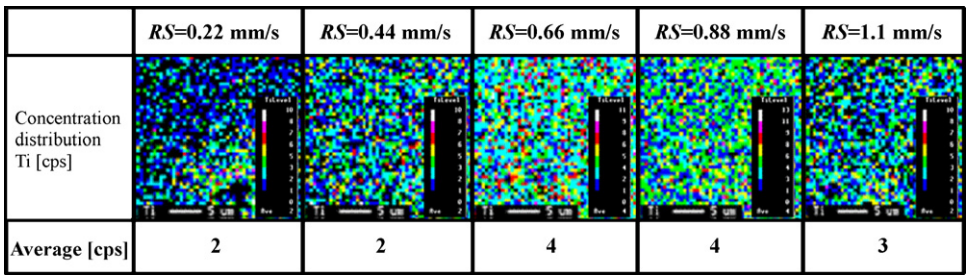

Fig. 7. EPMA images of TiO_2 film prepared under conditions of different several *RS*.

TiO_2 film and the coated substrate in firing process becomes larger with the increase of *RS* since the temperature distribution in the thickness direction is occurred more easily. Therefore, clucks and gaps are formed easily under the higher *RS* conditions. It can be concluded that the general characteristics of TiO_2 film prepared by sol–gel and dip-coating method is confirmed in this study.

Fig. 7 demonstrates EPMA images of TiO_2 film prepared under different several *RS* conditions. These EPMA images are taken by 1500 times magnification under the condition of acceleration voltage of 15 kV and current of 3.0×10^{-8} A. In Fig. 7, the concentration distribution of Ti in observation area is indicated by the difference of color. Light colors, e.g. white, pink and red mean that the amount of Ti is large, while dark colors like black, blue and green mean that the amount of Ti is small. EPMA detects the each element whose crystallization characteristic is memorized in advance. Therefore, if the large concentration of Ti is detected, it means that the amount of crystallized TiO_2 coated on gas separation membrane is large.

The averaged concentration of Ti in the observation area is also shown in Fig. 7. From this figure, the averaged concentration of Ti becomes larger with the increase in *RS* from 0.22 mm/s to 0.88 mm/s. Consequently, it can be known that the increase in *RS* brings the thickness of TiO_2 film and the large amount of TiO_2 film. However, the increase in averaged concentration of Ti is not confirmed when *RS* is set too high. Comparing EPMA images with SEM images shown in Fig. 8, it can be seen clearly that the high and low concentration area of Ti in EPMA images is observed in the white and black area in SEM images taken by 1500 times magnification, respectively. TiO_2 film is contracted by thermal stress acted on the interface between TiO_2 film and gas separation membrane in the firing process, resulting that large gaps are formed. In Fig. 8, the concentration of Ti shown as the black area in SEM images is 0 cps, while the concentration of Ti shown as the white area in SEM images ranges between 1 cps and 18 cps. The averaged concentration of Ti for *RS* = 1.7 mm/s, 2.2 mm/s, 3.3 mm/s is 2 cps, 3 cps, and 3 cps, respectively. Consequently, it can be known that the average concentration of Ti under the high *RS* conditions becomes small relatively.

The above results demonstrate that the promotion of CO_2 reforming performance can be expected when *RS* is in the range between 0.22 mm/s and 1.1 mm/s, because the TiO_2 films made from the *RS* in this range have large reaction surface area as well as increased amount of coated TiO_2. However, further increasing *RS*, e.g. from 1.1 mm/s to 2.2 mm/s would decrease reaction surface areas of TiO_2 film.

3.2. CO_2 reforming by the membrane reactor of batch type

Fig. 9 shows the CO concentration change in products with illumination time of UV light for several TiO_2 films prepared under conditions of different *RS*. According to our previous studies, the reversal of superiority or inferiority on CO_2 reforming performance of TiO_2 film among selected parameters was confirmed until UV light illumination time of 48 h. However, this reversal was not confirmed and the superiority or inferiority among selected parameters was kept after UV light illumination time of 78 h.

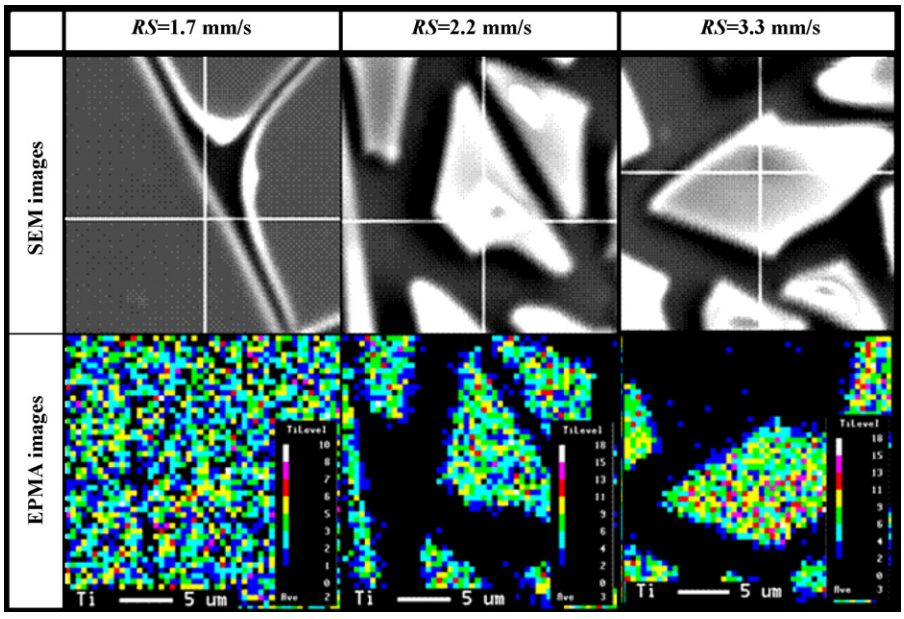

Fig. 8. Comparison between EPMA images and SEM images.

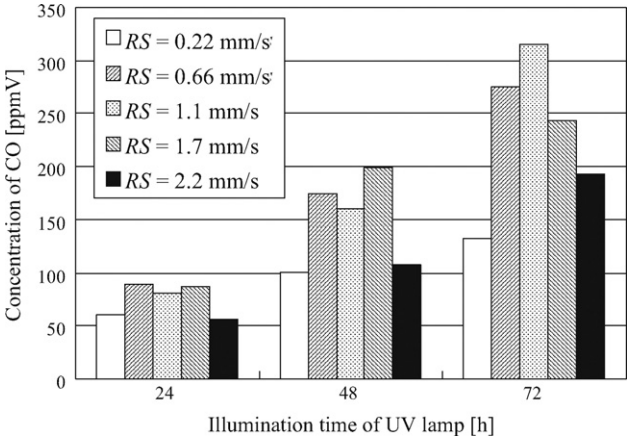

Fig. 9. Concentration change in produced CO with illumination time of UV light for several TiO_2 film prepared under conditions of different *RS*.

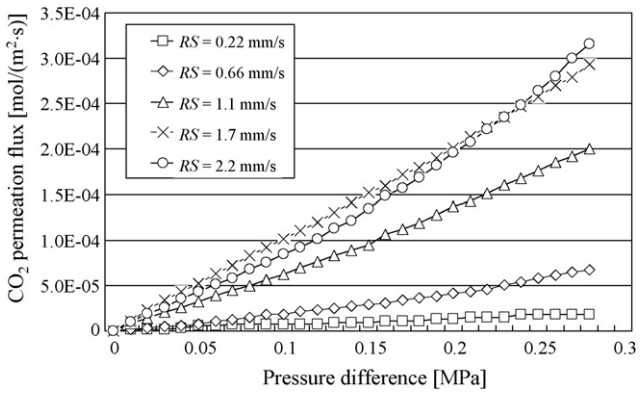

Fig. 11. Relationship between CO_2 permeation flux and pressure difference for several TiO_2 film prepared under conditions of different *RS*.

From this reason, I discuss the best condition for promotion of CO_2 reforming performance with using the data obtained under UV light illumination time of 78 h. From Fig. 9, it is known that the concentration of CO is increased with the films made from higher *RS* values up to 1.1 mm/s. However, the concentration of CO is decreased when *RS* is over 1.1 mm/s. Referring to the images of the SEM and EPMA shown in Figs. 6–8, the reason of this is thought to be that the amount of TiO_2 coated on gas separation membrane becomes larger when *RS* increases within the range of 0.33–1.1 mm/s, then the amount would not increase longer when *RS* becomes bigger. Instead gaps become larger compared with *RS* = 1.1 mm/s. Expansion of gaps area means the reduction in the reaction surface area of TiO_2 film. Although the averaged concentration of Ti is almost same, the CO_2 reforming performance for the films made from the *RS* beyond the value of 1.1 mm/s decreases due to the expansion of gaps area.

According to the reaction scheme [1,5,8,14,28,29,31,35–39] shown in Fig. 10, the number of electron and hydrogen ion (H^+) decides what products can be produced in the reaction. In this experiment, CH_4 and C_2H_4 and the other hydrocarbons were not detected by gas chromatograph, due to less H^+ in the reaction. Therefore, the amount of water vapor injected into the reactor will be the next parameter to be investigated since it is the source of H^+. From the reaction scheme, water vapor of 1 mol to CO_2 of 1 mol is necessary to produce CO of 1 mol. In this study, the amount of substance of injected water and CO_2 charged in the batch type reactor is 55.6 mmol and 13.0 mmol, respectively, resulting that the molar ratio of water vapor to CO_2 is 4.28. Although the amount of water vapor injected seemed sufficient for this reaction, we are to check the change in temperature distribution and the concentration distribution of water vapor in the batch type reactor with time, in our future research. Another point that can be confirmed from the experiment is that the metal deposition on TiO_2 film coated on gas separation membrane has positive effect on the reduction performance of CO_2. Deposited metal can supply electron and prevent the recombination of electron and hole which are produced by photocatalytic reaction [40,41].

3.3. CO_2 permeation by the membrane reactor of batch type

Fig. 11 shows the relationship between CO_2 permeation flux and pressure difference for several TiO_2 films prepared under conditions of different *RS*. The pressure difference is calculated by subtracting the pressure after penetrating the gas separation

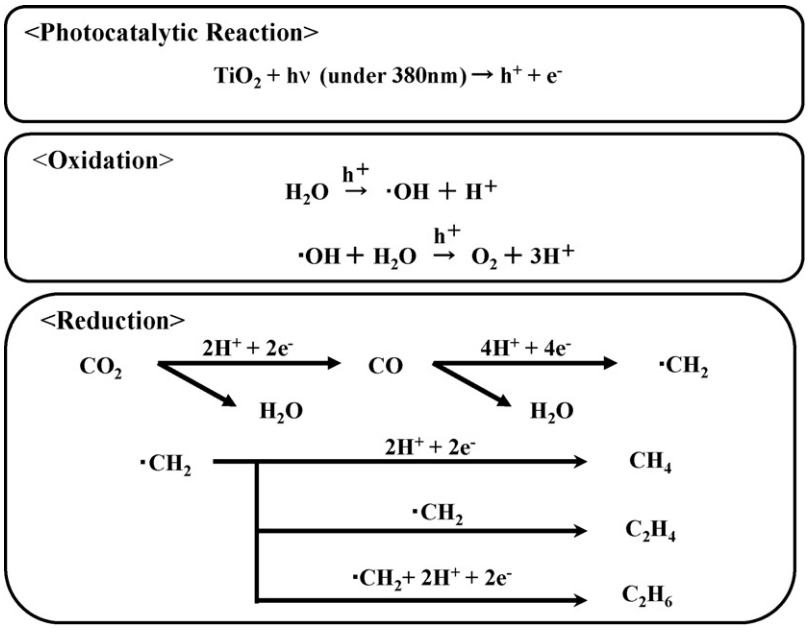

Fig. 10. Reaction scheme of CO_2 reforming into fuel by TiO_2 photocatalyst.

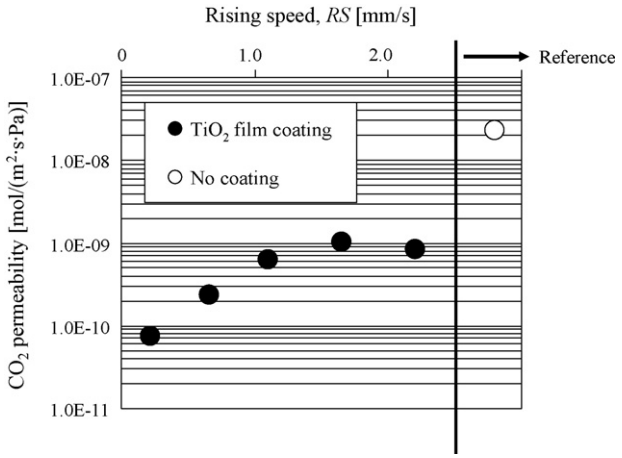

Fig. 12. CO_2 permeability for several TiO_2 film prepared under conditions of different *RS* including no coating.

membrane from the gas pressure before. CO_2 permeation flux is calculated by the following equation:

$$F_{CO_2} = \frac{V_p}{A_p t_p} \quad (1)$$

where F_{CO_2}, V_p, A_p and t_p are CO_2 permeation flux [mol/(m^2 s)], volume of permeated gas [mol], outer surface area of gas separation membrane [m^2] and gas penetration time [s], respectively.

Comparing these results at pressure difference of 0.28 MPa, it is known that CO_2 permeation flux is increased for the films with higher *RS* values. CO_2 permeation performance is down for the films with *RS* value between 0.22 mm/s and 0.66 mm/s since TiO_2 film may block the pores openings of gas separation membrane. On the other hand, CO_2 permeation performance for the film with *RS* values between 1.7 mm/s and 2.2 mm/s, becomes higher than others because large gaps are formed in TiO_2 film as shown in Fig. 6.

To evaluate the degree of pores blocked by TiO_2 film coating, Fig. 12 shows the CO_2 permeability for several TiO_2 film prepared under conditions of different *RS* including no coating. CO_2 permeability is calculated by Eq. (2):

$$Q_{CO_2} = \frac{F_{Co_2}}{P_s - P_p} \quad (2)$$

where Q_{CO_2}, P_s and P_p means CO_2 permeability [mol/(m^2 s Pa)], pressure of gas supplied to gas separation membrane [Pa] and pressure of gas after penetrating gas separation membrane [Pa], respectively.

From Fig. 12, it can be seen that CO_2 permeability of gas separation membrane with TiO_2 film is in the range between 7.4×10^{-11} mol/(m^2 s Pa) and 1.0×10^{-9} mol/(m^2 s Pa), while CO_2 permeability of gas separation membrane without TiO_2 film is 2.3×10^{-8} mol/(m^2 s Pa). According to these results, it is known that CO_2 permeability of gas separation membrane without TiO_2 coating is about 20–300 times higher than that of the gas separation membrane with TiO_2 coating.

3.4. Selection of the optimum coating condition

To select the optimum coating condition of coating the TiO_2 film on gas separation membrane which would lead to the highest CO_2 reforming and permeation performance, the results by SEM and EPMA and the results of CO_2 reforming and permeation experiment by the batch type reactor are compared and analyzed. Fig. 13 shows the comparison of the results between the concentration of produced CO and the CO_2 permeation flux for various *RS* conditions. In Fig. 13, the concentration of CO after UV illumination of 72 h and CO_2 permeation flux at pressure difference of 0.28 MPa are shown. It can be seen that CO_2 permeation flux is increased with increase in *RS* gradually. On the other hand, the concentration of CO is also increased with the increase of *RS* up to 1.1 mm/s and then decreased after *RS* is over 1.1 mm/s. In addition, it can predict that the reaction surface area of TiO_2 film would decrease when *RS* is over 2.2 mm/s due to occurrence of larger gaps as shown in Fig. 6. From this analysis, it can be concluded that *RS* equal to 1.1 mm/s is the optimum value and TiO_2 film coated under this *RS* gives the highest CO_2 reforming performance. According to Fig. 13, the CO_2 permeation flux peaks when *RS* equals 2.2 mm/s but is only 1.4 times as large as that when *RS* equals 1.1 mm/s. Consequently, *RS* equal to 1.1 mm/s is selected as the optimum coating condition for the best CO_2 reforming performance. The results shown and discussion below in Section 3.5 are all under this optimum condition.

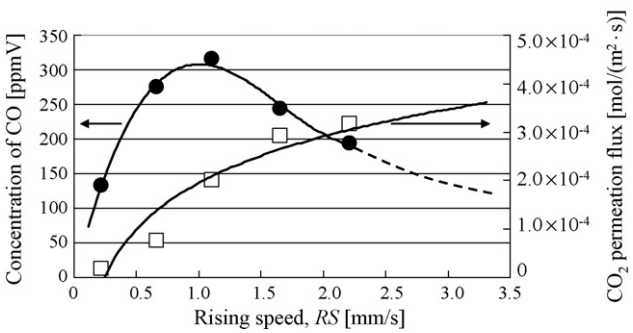

Fig. 13. Comparison of the results between concentration of produced CO and CO_2 permeation flux for each condition.

3.5. CO_2 reforming by the membrane reactor of gas circulation type

According to the reaction scheme shown in Fig. 10, CO is re-oxidized with the O_2 that is a by-product in this reaction, after attaining to the steady reaction state, resulting that the concentration of CO is decreased. This is the opposite reaction toward CO_2 reforming into fuel. Moreover, since the photocatalyst reaction occurred on the reaction surface, it is easy for the reaction surface to be covered by the products, which would stop the further reaction to happen. Therefore, removing the product of CO and CH_4 from the reaction surface as well as transporting the reactants, i.e. CO_2 and water vapor to the reaction surface quickly are necessary to promote further reaction and prevent the re-oxidization of CO. In this study, tube pump and gas separation membrane are used to realize this desirable measure for the promotion of CO_2 reforming performance.

Fig. 14 shows the concentration change in produced CO with illumination time of UV light. To show the effect of gas separation and circulation on the CO_2 reforming performance, the gas circulation by the tube pump only starts after the steady reaction state is reached. The steady reaction state was defined as the state without further increase in concentration of CO with time. Since the concentration of CO is diluted with the CO_2 in the pipe lines of the gas circulation type reactor after starting gas circulation, the concentration of CO is corrected by the following equation:

$$C_c = \frac{V_{total} C_d}{V_{batch}} \quad (3)$$

where C_c, V_{total}, C_d, and V_{batch} mean corrected concentration of CO [ppmV], total gas volume inside the experimental apparatus including the gas volume in the pipe lines [m^3], detected concentration of CO [ppmV], and total gas volume inside the

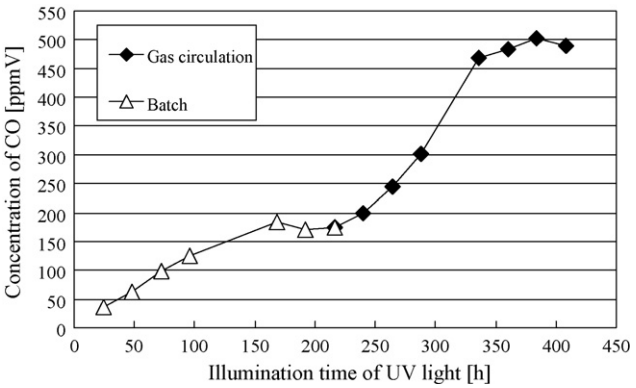

Fig. 14. Concentration change in produced CO with illumination time of UV light.

experimental apparatus in the case of batch type reactor [m^3], respectively.

The experiment by batch type and gas circulation type was carried out during the period from 0 h to 216 h and from 216 h to 408 h, respectively. It is observed that the concentration of CO in the reactor keeps increasing until 168 h and starts decreasing slightly after 168 h. The highest concentration of CO which is 183 ppmV is obtained at 168 h after illuminating UV light. Therefore, it is determined that the experiment by batch type reactor attains to the steady reaction state at 168 h.

After gas circulation, the concentration of CO starts to increase again, and picked at 502 ppmV at UV light illumination of 384 h. Consequently, the positive effect of gas separation and circulation on CO_2 reforming performance is confirmed. Although the concentration of product is still lower comparing with the previous studies [27–31], the study of using metal deposition on TiO_2 film coated on gas separation membrane to promote the reduction reaction further and get the synergism between them is being undertaken.

To show that the steady reaction state and inverse reaction have occurred or not clearly, the change in production rate of CO with illumination time of UV light is shown in Fig. 15. Production rate of CO can classify the reaction state into progressive, steady and inverse reaction state by positive, 0 and negative value, respectively. In Fig. 15, there is no data bar shown for the period from 96 h to 144 h and from 288 h to 312 h due to missing data. The production rate of CO, in Fig. 15, which is calculated by Eq. (4):

$$R_{CO} = \frac{C_c}{t_{int}} \quad (4)$$

where R_{CO} and t_{int} means production rate of CO [ppmV/h] and gas sampling interval [h], respectively. The t_{int} used for calculating R_{CO} is 24 h.

In the experiment in batch type reactor, it can be seen that the production rate of CO attains to the peak which is 1.5 ppmV/h at the UV light illumination of 24 h and is decreased afterwards gradually. The negative production rate of CO means the inverse reaction, i.e. re-oxidization occurring during the period from 168 to 192 h. In the experiment with gas circulation type reactor, the production rate of CO keeps increasing with increase in illumination time of UV light just after starting the gas circulation, resulting that it peaks at the highest value of about 3.5 ppmV/h for the period from 312 h to 336 h. However, the production rate of CO became lower after the passage time of 120 h, i.e. after total illumination time of UV light of 336 h.

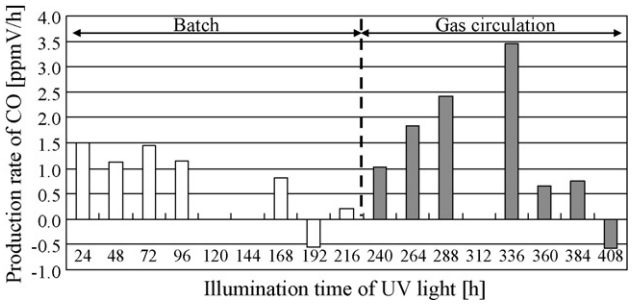

Fig. 15. Change in produced rate of CO with illumination time of UV light.

Since the production rate of CO just after starting the gas circulation increases significantly comparing to that at the beginning of the batch type experiment, it demonstrated the effectiveness of removing the products from the reaction surface and transport the reactants to the reaction surface. Consequently, it shows that using gas separation membrane to prevent the steady reaction state and reverse reaction from happening works.

4. Conclusions

Based on the above experimental results and discussion, the following conclusions can be drawn.

(I) The uniform coating is achieved for TiO_2 film if the *RS* values are below 0.22 mm/s, during the preparation. The cluck is formed and increased with in higher *RS* values, between *RS* = 0.33 mm/s and *RS* = 1.1 mm/s. The gap size is also increased with increase in *RS* when TiO_2 film is prepared over *RS* = 1.1 mm/s.

(II) The averaged concentration of Ti becomes larger with the increase of *RS* from *RS* = 0.22 mm/s to *RS* = 0.88 mm/s. However, it may not be the case when *RS* is set over 1.7 mm/s.

(III) *RS* equal to 1.1 mm/s is selected as the optimum coating condition since the best CO_2 reforming performance as well as the nearly best CO_2 permeation performance is obtained under this condition. The CO_2 reforming and permeation performance in the experiment with the batch type reactor agrees with the results of SEM and EPMA analysis.

(IV) With the usage of tube pump and gas separation membrane, the concentration of CO has increased after the steady reaction state in the batch type reactor. The production rate of CO at the point of starting the gas circulation is even higher than that at the starting of the batch type experiment, which demonstrates the effectiveness of preventing the steady reaction state and reverse reaction from happening by using this membrane reactor system, coated with TiO_2 on CO_2 reforming into fuel.

Acknowledgements

This work is financially supported by the Association for the Progress of New Chemistry, and Grant-in-Aid for Young Scientists (B) (20760605) in Japan.

References

[1] T. Inoue, A. Fujishima, S. Konishi, K. Honda, Nature 277 (1979) 637.
[2] B. Aurian-Blajeni, M. Halmann, J. Manassen, Solar Energy 25 (1980) 165.
[3] A. Henglein, M. Gutierrez, Ber. Bunsenges. Phys. Chem. 87 (1983) 852.
[4] M. Anpo, K. Chiba, J. Mol. Catal. 74 (1992) 207.
[5] K. Hirano, K. Inoue, T. Yatsu, J. Photochem. Photobiol. A: Chem. 64 (1992) 255.
[6] K. Ogura, M. Kawano, J. Yano, Y. Sakata, J. Photochem. Photobiol. A: Chem. 66 (1992) 91.
[7] O. Ishitani, C. Inoue, Y. Suzuki, T. Ibusuki, J. Photochem. Photobiol. A: Chem. 72 (1993) 269.
[8] K. Adachi, K. Ohta, T. Mizuno, Solar Energy 53 (1994) 187.
[9] K. Takeuchi, S. Murasawa, T. Ibusuki, World of Photocatalyst, vol. 29, Kougyouchousakai, Tokyo, 2001, p. 148.
[10] S. Kaneco, H. Kurimkoto, Y. Shimizu, K. Ohta, T. Mizuno, Energy 24 (1999) 21.
[11] G.R. Dey, A.D. Belapurkar, K. Kishore, J. Photochem. Photobiol. A: Chem. 163 (2004) 503.
[12] C.C. Lo, C.H. Hung, C.S. Yuan, J.F. Wu, Solar Energy Mater. Solar Cells 91 (2007) 765.
[13] M. Halmann, V. Katzir, E. Borgarello, J. Kiwi, Solar Energy Mater. 10 (1984) 85.

[14] Z. Goren, I. Willner, A.J. Nelson, A.J. Frank, J. Phys. Chem. 94 (1990) 3784.
[15] T. Ibusuki, Syokubai 35 (1993) 506.
[16] K. Kawano, T. Uehara, H. Kato, K. Hirano, Kagaku to Kyoiku 41 (1993) 766.
[17] H. Yamashita, H. Nishiguchi, N. Kamada, M. Anpo, Res. Chem. Intermed. 20 (1994) 815.
[18] I.H. Tseng, W.C. Chang, J.C.S. Wu, Appl. Catal. B: Environ. 37 (2002) 37.
[19] X.H. Xia, Z.J. Jia, Y. Yu, Y. Liang, Z. Wang, L.L. Ma, Carbon 45 (2007) 717.
[20] J. Qu, X. Zhang, Y. Wang, C. Xie, Electrochem. Acta 50 (2005) 3576.
[21] P. Pathak, M.J. Meziani, Y. Li, L.T. Cureton, Y.P. Sun, Chem. Commun. (2004) 1234.
[22] F. Cecchet, M. Alebbi, C.A. Bignozzi, F. Paolucci, Inorg. Chim. Acta 359 (2006) 3871.
[23] L.F. Cueto, G.A. Hirata, E.M. Sanchez, J. Sol–Gel Sci. Technol. 37 (2006) 105.
[24] J.C.S. Wu, H.M. Lin, Int. J. Photoenergy 7 (2005) 115.
[25] O. Ozcan, F. Yukruk, E.U. Akkaya, D. Uner, Top. Catal. 44 (2007) 523.
[26] Y. Sasaki, K. Asano, Sozai Busseigaku Zasshi 20 (2007) 1.
[27] A. Nishimura, N. Sugiura, S. Kato, N. Maruyama, S. Kato, AIAA Meeting Papers on Disc of 2nd International Energy Conversion Engineering Conference, 16–19 August, AIAA, 2004, p. 5619.
[28] A. Nishimura, N. Sugiura, M. Fujita, S. Kato, S. Kato, Kagaku Kogaku Ronbunshu 33 (2007) 146.
[29] A. Nishimura, N. Sugiura, M. Fujita, S. Kato, S. Kato, Kagaku Kogaku Ronbunshu 33 (2007) 432.
[30] A. Nishimura, M. Fujita, S. Kato, in: Proceedings of the 6th Asia Pacific Conference on Sustainable Energy and Environmental Technologies, 7–11 May, 2007.
[31] A. Nishimura, N. Sugiura, M. Fujita, S. Kato, AIAA Meeting Papers on Disc of 3rd International Energy Conversion Engineering Conference, 15–18 August, AIAA, 2005, p. 5536.
[32] S. Himeno, Nagaoka University Techno-Incubation Center News (2005) 6.
[33] http://cosmobio.co.jp/product/product_MEK_20041026_08.asp.
[34] T. Nakagawa, Hyoumen 26 (1988) 506.
[35] Y. Hori, K. Kikuti, S. Suzuli, Chem. Lett. (1985) 1965.
[36] R. Maidan, I. Willner, J. Am. Chem. Soc. 108 (1986) 8100.
[37] K.R. Thampi, J. Kiwi, M. Gratzel, Nature 327 (1987) 506.
[38] I. Willner, R. Maidan, D. Mandler, H. Durr, G. Dorr, K. Zengerle, J. Am. Chem. Soc. 109 (1987) 6080.
[39] M. Anpo, Res. Chem. Intermediates 11 (1989) 67.
[40] T. Ibusuki, K. Tabata, Syokubai 39 (1997) 24.
[41] Y. Nosaka, A. Nosaka, Introduction of Photocatalyst, 1st ed., Tokyotosho, Tokyo, 2004, p. 151.